SECOND EUROPEAN CONFERENCE ON EARTHQUAKE ENGINEERING AND SEISMOLOGY, ISTANBUL AUG. 25-29, 2014

FRAGILITY ANALYSIS OF BUCKLING-RESTRAINED BRACED FRAMES AT NEAR-FAULT SITES

Ahmad Fayeq GHOWSI[1] and Dipti Ranjan SAHOO[2]

ABSTRACT

Buckling-restrained braced frames (BRBFs) are primarily used as lateral force-resisting systems in the structures. BRBFs consist of buckling-restrained braces (BRBs) arranged in various configurations, such as, Inverted-V (Chevron) and Double-story-X along their heights. Past studies focus on the behaviour of BRBFs under the far-field earthquake conditions and hence, there is a need to investigate the seismic response of BRBFs under the near-field ground motions. In this study, the effect of brace configuration on the overall seismic response of a medium-rise BRBF under near-field ground motions have been analytically evaluated for a seven-story steel building in which all braced bays are located along its exterior perimeter. Nonlinear dynamic analyses are carried out for an ensemble of forty SAC ground motions representing the near-fault records. Fragility curves are developed using log-normal probability distribution function. Interstory drift (ISDR) and residual drift (RDR) response are considered as Engineering Demand Parameters in the fragility analysis. The maximum ISDR response is noted at the first and seventh story level, whereas the maximum RDR response is noted at the seventh story level of the BRBF. Further, the drift response is smaller at a story level where the rigid beam-column connections are used. Both RDR and ISDR response of BRBFs designed as per the current code provisions exceeded the 2% limit corresponding to the "collapse prevention" performance objective as specified in FEMA356 (2000) under the near-fault ground motions.

INTRODUCTION

Buckling-restrained braced frames (BRBFs) are primarily used as lateral force-resisting systems in the structures located in the seismically-active regions. Buckling-restrained braces (BRBs) are the main elements intended to undergo the inelastic axial deformations under cyclic loading. Fig. 1(a) shows the different components of a BRB element. Steel core plates of BRBs are encased by unbonded concrete/mortar inside a steel casing. Since the compression buckling of BRBs is restrained by the encasing material, the yielding of BRBs in tension and compression results in a symmetric hysteretic response, higher ductility level, and excellent energy dissipation as shown in Fig. 1(b). A number of tests at the component level as well as the system level have been conducted by various researchers to investigate the seismic performance of BRBFs (e.g., Watanabe et al. 1988; Aiken et al. 2002; Iwata et al. 2003; Merritt et al. 2003; Romero et al. 2003; Tsai et al. 2003; Black et al. 2004; Fahnestock et al. 2007; Chou et al. 2012). The main parameters studied are the displacement ductility and cumulative displacement ductility, energy dissipation potential, compression over-strength and strain-hardening factors, detailing of non-yielding segments and the end connections of BRBs. The type of beam-to-column connections and the arrangement of BRBs have a great impact on the seismic response of BRBFs (Field and Ko 2004; Lin et al. 2005; Fahnestock et al. 2007).

[1] Doctoral Candidate, Indian Institute of Technology Delhi, New Delhi, India, faieq.ghowsi@gmail.com
[2] Assistant Professor, Indian Institute of Technology Delhi, New Delhi, India, drsahoo@civil.iitd.ac.in

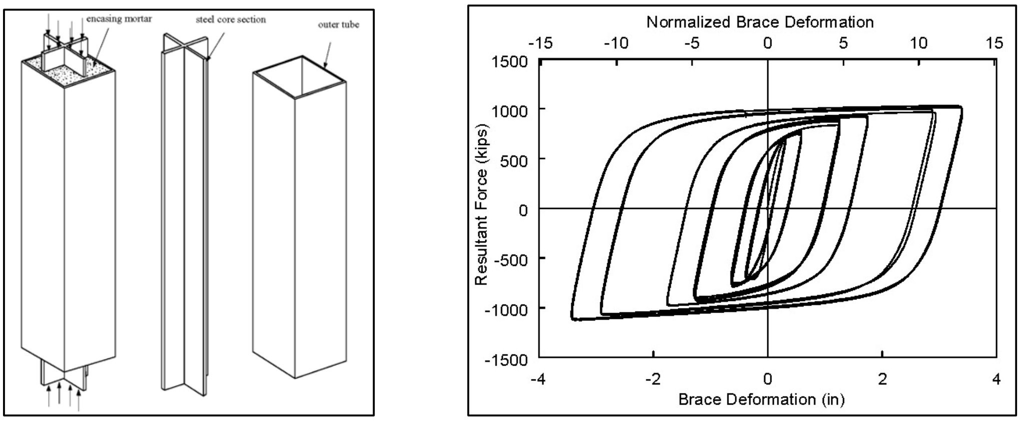

(a) (b)

Figure 1. (a) Components of an unbonded BRB (Black et al., 2004); (b) Typical hysteretic response of BRBs under cyclic loading (Merritt et al., 2003)

Beam-to-column connections in a BRBF can be of moment-resisting (rigid) or non-moment-resisting (pined) types. BRBs can also be arranged in Single-diagonal, Chevron (Inverted-V) or Double-story-X configurations. A recent study by Ghowsi and Sahoo (2013) concluded that Double-story-X configuration of BRBs resulted in the relatively larger post-earthquake residual drift response of BRBFs as compared to those in Chevron configuration. Further, although the pinned beam-to-column connections result in the smaller interstory drift response of BRBFs as compared to the rigid connections, the formation of plastic hinging in the intermediate columns may induce the soft-story collapse of BRBFs. Most of the past studies are focused on the seismic response of BRBFs under the far-field earthquakes. Very limited studies have been conducted on the performance of BRBFs under the near-field earthquakes (e.g., Baghbanijavid et al. 2010; Shakib and Safi 2012). The near-fault ground motions often contain strong dynamic long period pulses that may lead to the permanent ground displacements. The effects of thse ground motions are still not known and hence, are not included in the design spectrums of various international codes (e.g., ASCE/SEI 7-10, 2010). The past studies have shown that the near-fault ground motions can cause extensive structural damages as compared to the far-fault ground motions. Significant post-earthquake residual drift response can be expected in BRBFs, which may cause damage to the non-structural systems (Baghbanijavid et al. 2010). Hence, there is a need of further study to investigate the performance of BRBFs under near-fault earthquakes.

In this study, the effect of brace configurations on the overall seismic response of a medium-rise BRBF under the near-field ground motions has been analytically evaluated. The main objective of this study is to investigate the probability of exceeding the damage limits for the BRBFs equipped with both Chevron and Double-story-X BRBs. Nonlinear dynamic analyses are carried out under the selected near-fault seismic excitations to understand the structural and ground motion characteristics that influence their seismic behavior of BRBFs. Fragility curves are developed for peak interstory drift and residual drift response of BRBFs.

MODELING OF STUDY FRAMES

A seven-story steel building has been considered as the study building in which all braced bays are located along its exterior perimeter. The overall height of the building is 25.33 m with a typical story height of 3.51 m, except the first story of 4.27 m in height. The details of building geometry, loading, frame sections designed as per code provisions can be found elsewhere (López and Sabeli, 2004). The braced bay (of width 9.15 m) along the shorter direction of building is considered as the study frame. Two types of brace configurations (i.e., Chevron and Double-X) along with the combination of the moment-resisting and the non-moment-resisting beam-column connections are considered. In all cases, a constant value of response reduction (R) factor equal to 8 is used in the design of braces, which corresponds the BRBFs with pinned beam-column connections as per ASCE/SEI 7-10 (2010) provisions. Fig. 2 shows the details of the study frame considered in this study. In order to study the effect of brace configurations and type of beam-column connections, same structural sections are used as beams and columns in all BRBFs. All sections satisfy the seismic design requirements as per ANSI/AISC 341-05 (2005) provisions. The study frames are represented as CRBC, CPBC, XRBC, XPBC, and XAPBC, where “C” and “X” stand for “Chevron and Double-story-X BRB arrangements”, respectively, “RBC/PBC” represent “rigid/pined beam-column connections”, and “A” stands for “alternate floors”.

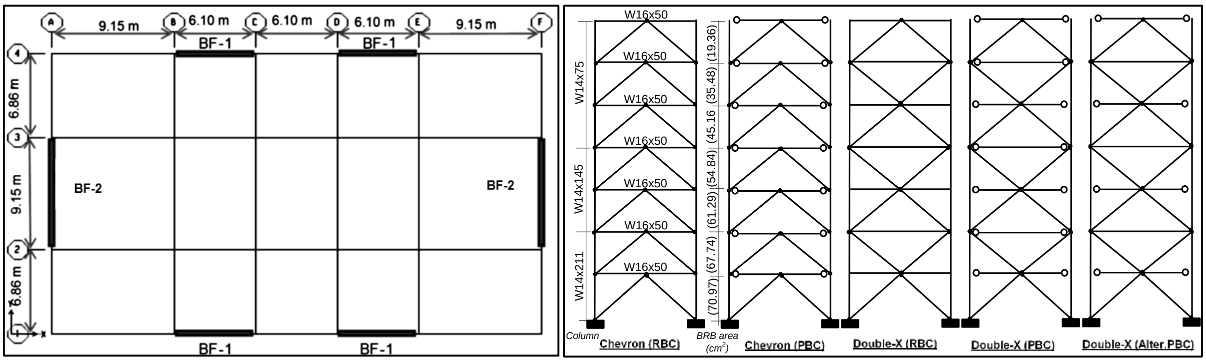

(a) (b)

Figure 2. (a) Plan view of the study building; (b) Elevation of BRBFs considered in this study

Nonlinear dynamic analysis of BRBFs is carried out using a computer software SAP2000 (CSI, 2009). All the beams and columns are modelled as frame elements capable of resisting the axial, shear, and bending actions. The elements are assigned the section and material properties. The value of tensile yield stress of steel used in BRBs, beams and columns is considered as 345 MPa. Material overstrength factor (R_y) for BRB is considered as unity. Compression overstrength (β) and strain-hardening (ω) factors of BRBs are assumed as 1.1 and 1.3, respectively. The nonlinear behaviour of frame members is considered in the models by using lumped plasticity concepts. Nonlinear moment-rotation (M-θ) plastic hinges along with the axial load-bending moment (P-M) interaction properties are assigned to all the columns and beams. Both (M-θ) and (P-M) plastic hinges are assigned at both end of the columns, whereas these properties are assigned at the mid-lengths of beams in addition to the ends in case of RBC connections.

Fig. 3(a) shows the nonlinear (M-θ) plastic hinge properties used in the frame members. Both moment and rotation values are normalized with respect to their corresponding yield values. The ultimate resistance is assumed as 15% of higher than the yield strengths. The post-peak residual strength is considered as 20% of the yield strengths. Axial force-displacement plastic hinges, as shown in Fig. 3(b), are used to model the nonlinear axial behaviour of BRBs. These plastic hinges are placed at the mid-lengths of BRBs. No post-peak descending behaviour is modelled for BRBs in this study. However, BRBs are assumed to have failed when the displacement ductility level exceeded a value of 25, the limit which most of the BRBs have exhibited in the past experimental studies (e.g., Fahnestock et al., 2007). Kinematic hardening behaviour is assumed for all the elements of BRBFs. P-Delta effect due to gravity loads is considered by modelling a leaning column pinned at its base and connected to the BRBFs through the rigid links at each floor level. The gravity loads contributing to the P-Delta effect are applied to the nodes at each floor level of the leaning column. All the columns of BRBFs are assumed to be fixed at their bases.

An ensemble of forty SAC ground motions representing the near-fault records (Somerville et al., 1997) are used in this study for the nonlinear dynamic analysis. Twenty ground motions (NF01-20) represent the recorded near-fault ground motions, whereas the remaining (NF21-40) ground motions are obtained by physical simulations considering the variations in the source-to-site distance (<20 km), fault rupture mechanism, soil medium, and earthquake magnitudes, etc., resembling the seismic characteristics in the near-fault region. Fig. 4(a) show the elastic acceleration spectrum of the input ground motions for 5% damping which shows the pulse-like and long-period characteristics of the ground motions. Fig. 4(b) shows a comparison of the average acceleration spectrum of all ground motions with the design spectrum as per ASCE/SEI 7-10 (2010). Except for the short period (<0.2 sec.), the average value of spectral acceleration of all ground motions lies well-above the design spectrum.

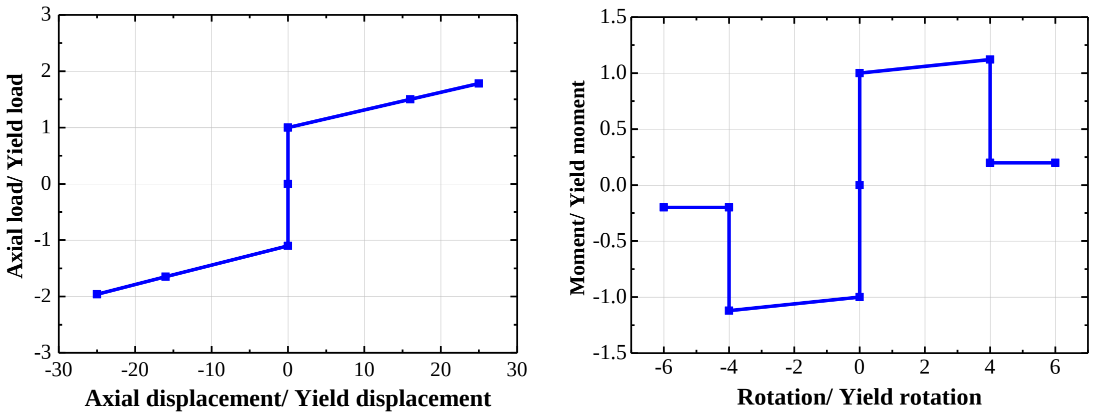

(a) (b)

Figure 3. (a) Plastic hinge properties of BRBs; (b) Plastic hinge properties of beam and column

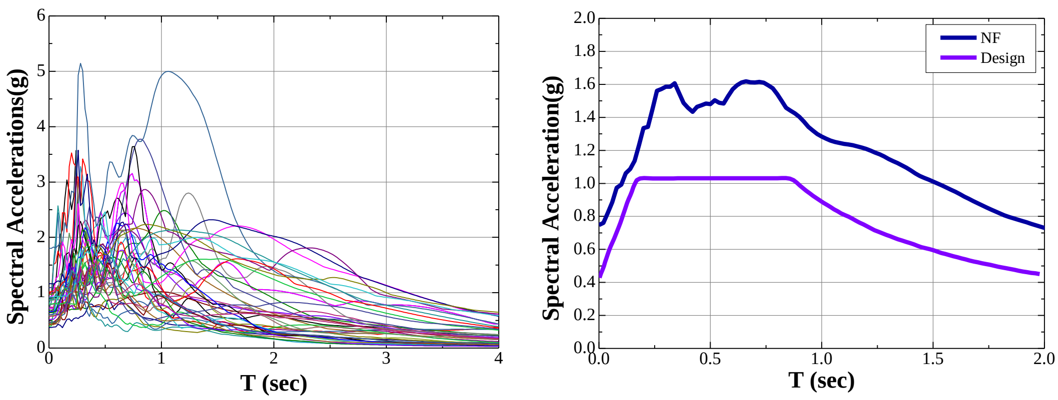

(a) (b)

Figure 4. (a) Elastic acceleration spectrum of the selected forty ground motions; (b) Comparison of average elastic acceleration spectrum with the design spectrum

FRAGILITY ANALYSIS

Fig. 5 show the plot between the number of occurrence and interstory drift response of a BRBF with Chevron brace arrangements considered in this study. The ISDR distribution plot is skewed towards the smaller drift values less than 1.5%. The number of occurrence rapidly decreases at the higher drift levels. Thus, log-normal probability density function has been considered for the fragility analysis in this study in which both mean (μ) and standard deviation (σ) values of the Engineering Demand Parameter (EDP) have been calculated for the selected earthquake records. A fragility curve represents the probability of reaching or exceeding a damage state at a specified seismic hazard level. The probability of exceedance (p) of each EDP, computed using a cumulative normal distribution function (ϕ), can be expressed as follows:

$$p(EDP > x) = 1 - F(\chi) = 1 - \phi\left(\frac{\ln(x) - \mu}{\sigma}\right), \qquad x > 0 \tag{1}$$

Where, $F(\chi)$ is the cumulative distribution function. Very often, drift response is used as an indicator of the damages in a structure. Hence, fragility curves have been developed for all study frames considering the interstory drift ratio (ISDR) and residual drift ratio (RDR) as the damage parameters. It is worth mentioning that other parameters, such as, Peak ground Acceleration (PGA), Spectral acceleration, etc., have also been used as the EDP by various researchers in the fragility analysis of structures.

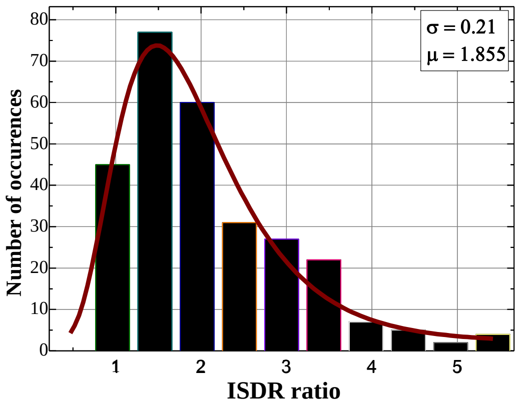

Fig. 5. Distribution of interstory drift response of CRBC frame considered in this study

Fig. 6 shows the fragility curves for the average value of peak ISDR and RDR response of BRBFs under forty near-fault earthquakes. BRBFs with Chevron brace configurations exhibited a steep slope of probability of exceedance varied form 0-100% for the peak ISDR values in the range of 4.0-6.5%. A 50% probability of exceedance is noted at the ISDR value of 5%. In case of BRBFs with Double-X BRB configurations, the probability of exceedance curve gradually varied from 0% at the ISDR value of 2% to a value of 100% at 7% ISDR level. Both brace configurations showed the same 70% probability of exceeding the ISDR value of 5.3%. The probability of exceedance is little higher for BRBFs with the Double-X braces as compared to the Chevron braces for a peak ISDR value less than 5.3% and vice versa. However, no significant difference in the fragility curves is noted for different types of beam-to-column connections. Hence, the type of BRB configurations in BRBFs played an important role in controlling the peak ISDR response. Fig. 6(b) shows the fragility curves for the peak RDR response of BRBFs under the selected ground motions. BRBFs with PBC connections exhibited the higher RDR response in both types of brace configurations. The probability of exceeding the RDR value of 2% is noted as 100% for BRBFs with Chevron brace configurations, whereas the corresponding value is found to be about 40% for the BRBFs with Double-X BRBs. The peak RDR response exceeded 2% for more than 75% of the selected ground motions. Unlike the ISDR response, the fragility curves for the RDR response of BRBFs are similar in both Chevron and Double-X BRB configurations. However, the higher value of RDR response of BRBFs is noticed if the BRBs are arranged in the Chevron configurations. Thus, both RDR and ISDR response of all BRBFs exceeded the 2% limit corresponding to the “collapse prevention” performance objective as specified in FEMA 356 (2000).

Fig. 7 shows the ISDR and RDR response at all story levels of BRBFs with Chevron BRB configurations with all RBC connections. The probability of exccedance the peak ISDR response is higher at the first story level up to 2% drift level, beyond which the higher probability of exceedance of ISDR is noted at the seventh story level. However, the higher probability of exceedance noted at the seventh floor level at all RDR values. Further, the smaller drift response is observed between second and fifth story level. Hence, the ground and top story levels of BRBFs are critical for the drift response in case of Chevron BRB arrangements with rigid beam-column connections at the near-fault site. Fig. 8 shows the ISDR and RDR response at various story levels of BRBFs with Chevron braces and PBC connections. The maximum probability of exceedance is noted for ISDR response at the first story level up to 2.6% drift level, beyond which the maximum probability of exccedance in ISDR response was noted at the seventh story level. However, the same probability of exccedance in the RDR response is noted at all the story levels of the BRBF. Fig. 9 shows the ISDR and RDR response of BRBFs with Double-X braces with RBC connections. The maximum probability of exceedance in ISDR response is noted at the first story level up to 2.3% drift level. Further, the higher values of both ISDR and RDR response is noted at the story levels where braces are connected at the center of the beam.

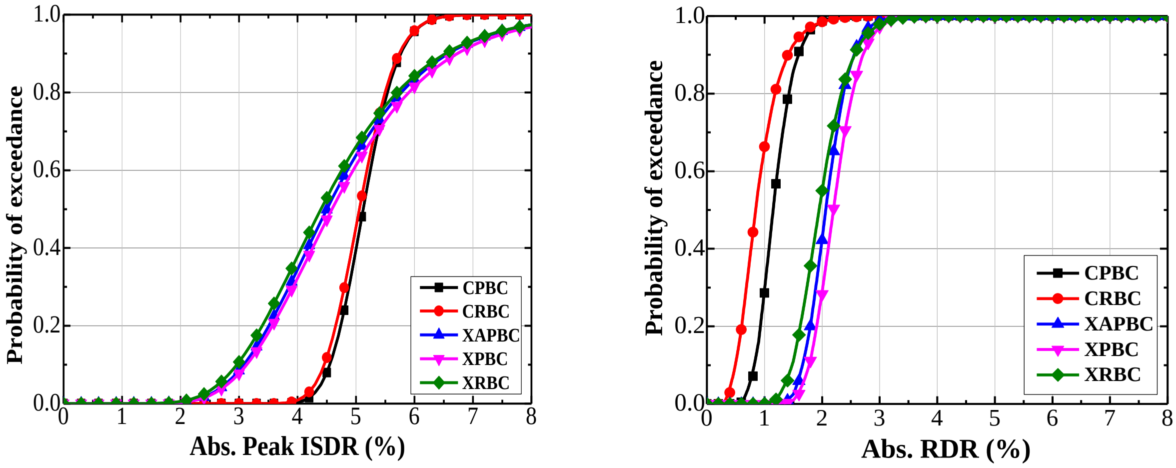

(a) (b)

Figure 6. Fragility curves for mean ISDR and RDR response of BRBFs

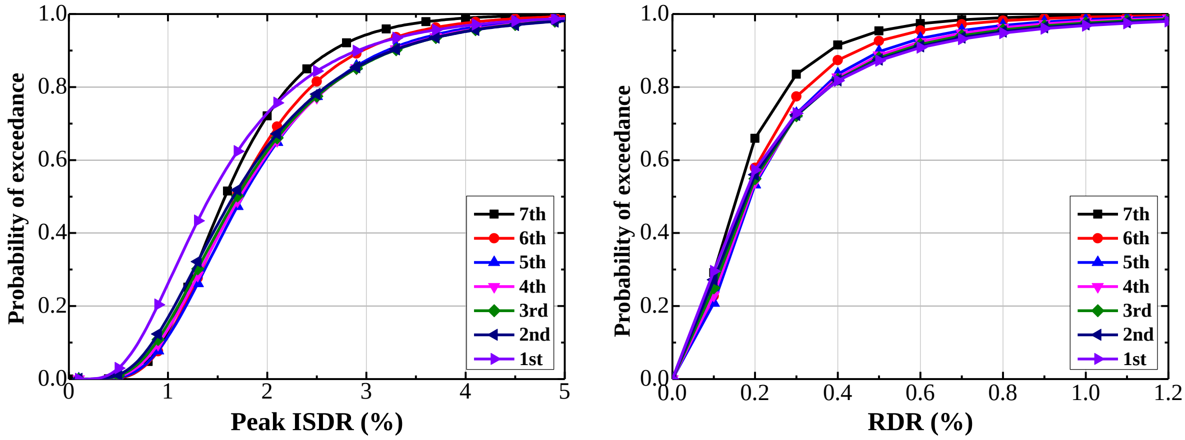

(a) (b)

Figure 7. Fragility curves for (a) ISDR and (b) RDR response of CRBC BRBF

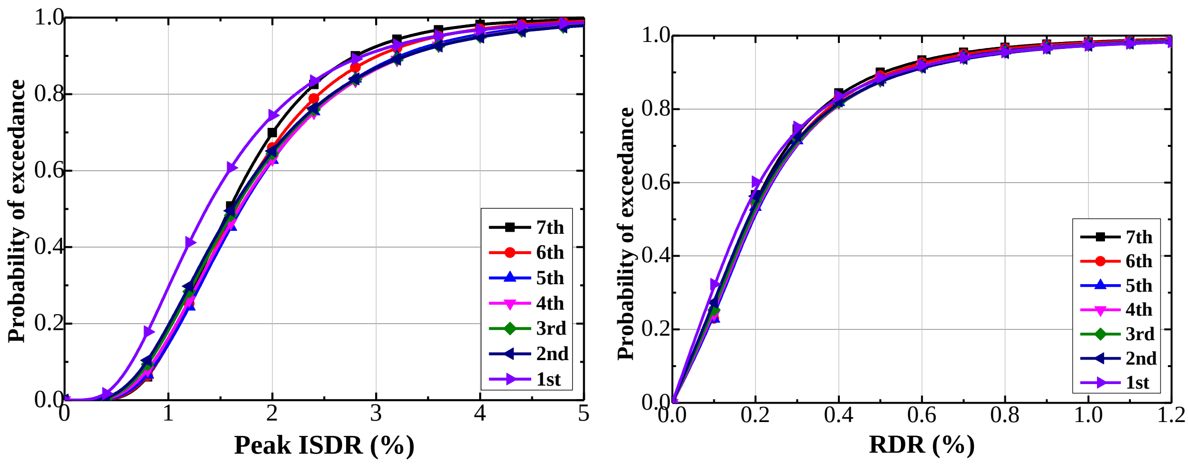

(a) (b)

Figure 8. Fragility curves for (a) ISDR and (b) RDR response of CPBC BRBF

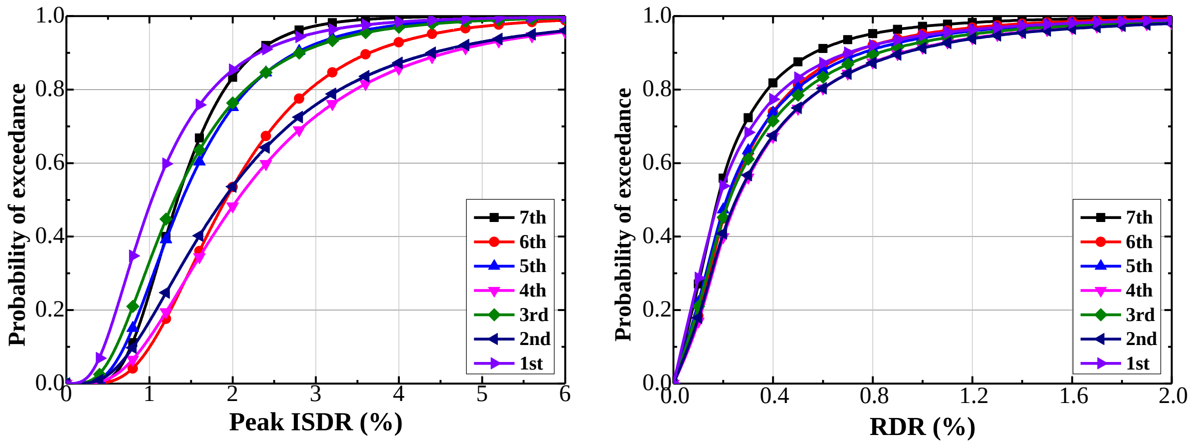

(a) (b)

Figure 9. Fragility curves for (a) ISDR and (b) RDR response of XRBC BRBF

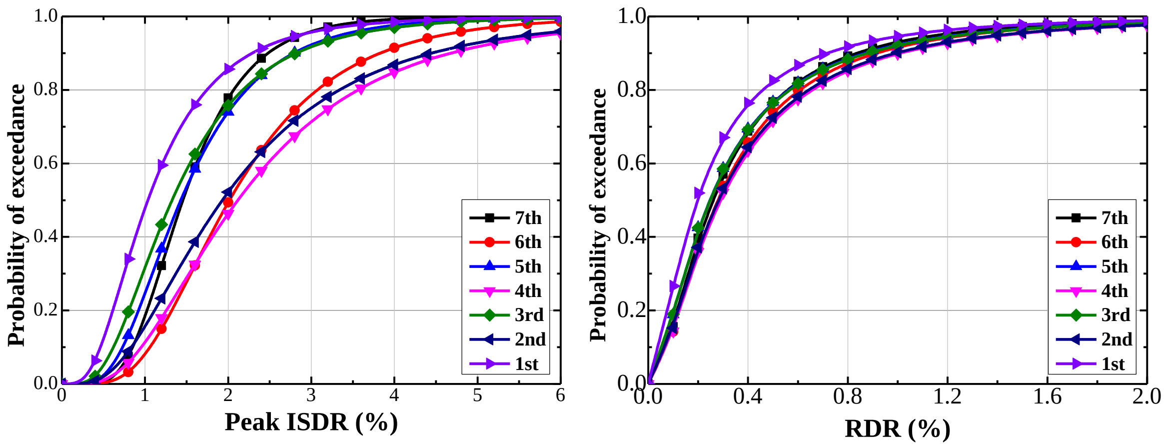

(a) (b)

Figure 10. Fragility curves for (a) ISDR and (b) RDR response of XPBC BRBF

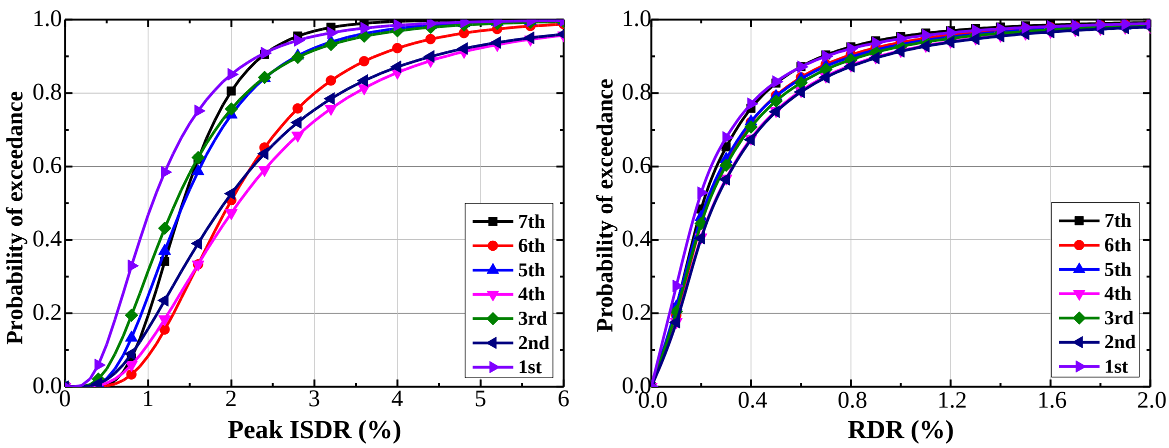

(a) (b)

Figure 11. Fragility curves for (a) ISDR and (b) RDR response of XAPBC BRBF

Fig. 10 shows the ISDR and RDR response at various story levels of BRBFs with Double-X braces with PBC connections. Both the maximum value of ISDR and RDR response is noted at the first story level. The probability of exceedance of ISDR and RDR response at different story levels of XAPBC BRBF is shown in Fig. 11. The maximum ISDR response is noted at the first story up to 2.4% drift level. No significant difference in the maximum RDR response is noted at various story levels of the BRBF.

In general, the RDR response of BRBF is reduced if the pined beam-to-column connections are used along with the BRBs arranged in Double-story-X configurations.

Conclusions

Based on the analysis results, following conclusions can be drawn for medium-rise BRBFs:

(1) Both RDR and ISDR response of BRBFs designed as per the current codes exceeded the 2% limit corresponding to the "collapse prevention" performance objective as specified in FEMA356 (2000) under the near-fault ground motions.

(2) The probability of exceedance of ISDR and RDR response of BRBFs is higher either at the first or seventh story level as compared those at the other stories in both Double-story-X and Chevron type of brace configurations.

(3) The RDR response of BRBF is reduced if the pined beam-to-column connections are used along with the BRBs arranged in Double-story-X configurations.

REFERENCES

Aiken ID, Mahin SA, Uriz PR (2002) "Large-scale testing of buckling restrained braced frames," *Proceedings of Japan Passive Control Symposium*, Tokyo Institute of Technology, Japan.

ANSI/AISC 341-05 (2005) Seismic provisions for structural steel buildings, American Institute of Steel Construction, Chicago, IL.

ASCE/SEI 7-10 (2010) Minimum design loads for buildings and other structures, American Society of Civil Engineers, VA.

Baghbanijavid Z, Jalali A, Yasrebinia Y (2010) "Seismic response of buckling-restrained braced frames under near fault ground motions," *Journal of Applied Sciences*, 10(23):2967-2977.

Black CJ, Makris N, Aiken ID (2004) "Component testing, seismic evaluation and characterization of buckling-restrained braces." *ASCE Journal of Structural Engineering*, 130(6), pp. 880-894.

Chou CC, Liu JH, Pham DH (2012) "Steel buckling-restrained braced frames with single and dual corner gusset connections: seismic tests and analyses," *Earthquake Engineering and Structural Dynamics*, 41(7), pp. 1137-1156.

CSI (2009) CSI Analysis Reference Manual for SAP 2000, Computers and Structures, Inc., Berkeley, CA.

Fahnestock LA, Sause R, Ricles JM (2007) "Seismic response and performance of buckling-restrained braced frames," *ASCE Journal of Structural Engineering*, 133(9), pp. 1195–1204.

FEMA 356 (2000) Prestandard and commentary for the seismic rehabilitation of buildings, Federal Emergency Management Agency, Washington, DC.

Field C, Ko E (2004) "Connection performance of buckling restrained braced frames," Paper No. 1321, *Proceedings of Thirteenth World Conference on Earthquake Engineering*, Vancouver, BC, Canada.

Ghowsi AF, Sahoo DR (2013) "Seismic performance of buckling-restrained braced frames with varying beam-column connections," *International Journal of Steel Structures*, 13(4):607-621.

Iwata M, Kato T, Wada A (2003) "Performance evaluation of buckling-restrained braces in damage-controlled structures: Behavior of steel structures in seismic area." *Proceeding of Fourth International Conference STESSA*, Naples, Italy.

Lin ML, Tsai KC, Hsiao PC, Tsait CY (2005) "Compressive behavior of buckling restrained braces gusset connections," *First International Conference on Advanced Experimental Structural Engineering*, Nagoya, Japan.

López WA and Sabelli R (2004) Seismic design of buckling-restrained braced frames. Structural Steel Education Council, Moraga, CA.

Merritt S, Uang CM, Benzoni G (2003) Subassemblage testing of corebrace buckling-restrained braces, Report No. TR-2003/01, Department of Structural Engineering, University of California at San Diego, USA.

Romero P, Reaveley L, Miller P, Okahashi T (2003) Full-scale testing of WC Series buckling-restrained braces, Department of Civil and Environmental Engineering, University of Utah, USA.

Shakib H, Safi R (2012) “Behavior evaluation of the eccentric buckling-restrained braced frames under the near-fault ground motions.” *Proceedings of Fifteenth World Conference on Earthquake Engineering*, Lisbon.

Somerville PG, Smith M, Punyamurthula S, Sun J (1997) Development of ground motion time histories for phase 2 of the FEMA/SAC Steel Project, Report No. SAC/BD-97/04, SAC Joint Venture, Sacramento, CA.

Tsai KC, Hsiaso BC, Lai JW, Chen CH, Lin ML, Weng YT (2003) “Pseudo-dynamic experimental response of a full-scale CFT-BRB composite frame,” *Proceedings of Joint NCREE/JRC Workshop on International Collaboration on Earthquake Disaster Mitigation Research*, Taipei, Taiwan.

Watanabe A, Hitomi Y, Saeki E, Wada A, Fujimoto M (1988) “Properties of brace encased in buckling-restrained concrete and steel tube.” *Proceedings of Ninth World Conference on Earthquake Engineering*, Tokyo, Japan.